Elucidation of the antiviral mechanism of natural therapeutic molecules Herbacetin and Caffeic acid phenethyl ester against Chikungunya and Dengue virus

Mandar Bhutkar[#], Ruchi Rani[#], Aditi Kothiala, Supreeti Mahajan, Bhairavnath Waghmode, Ravi Kumar, Vishakha Singh, Debabrata Sircar, Pravindra Kumar, Shailly Tomar*

Department of Biosciences and Bioengineering, Indian Institute of Technology Roorkee, Uttarakhand, India

[#] Both the authors have contributed equally

*Corresponding author address: Department of Biosciences and Bioengineering, Indian Institute of Technology Roorkee, Roorkee-247667, Uttarakhand, India; Email id: shailly.tomar@bt.iitr.ac.in

Abstract

Arthropod-borne viruses of the alphavirus and flavivirus genera are human pathogens of significant concern, and currently, no specific antiviral treatment is available for these viruses. In this study, the antiviral mechanisms of natural small molecules against Dengue virus (DENV) and Chikungunya virus (CHIKV) have been investigated. Herbacetin (HC) and Caffeic acid phenethyl ester (CAPE) showed depletion of polyamine levels in Vero cells as demonstrated by thin-layer chromatography (TLC). As polyamines are known to play a role in viral replication and transcription, HC and CAPE were expected to inhibit virus replication by reducing polyamine levels. To test this hypothesis, HC and CAPE were evaluated for antiviral activities using a cell-based virus yield assay by quantitative reverse transcription-polymerase chain reaction (qRT-PCR), plaque reduction assay, and immunofluorescence assay (IFA). HC and CAPE displayed potent inhibition with EC_{50} of 463 nM and 0.417 nM for CHIKV and 8.5 µM and 1.15 µM for DENV, respectively. Interestingly, however, the addition of exogenous polyamines did not completely rescue the virus titer in both CHIKV and DENV infected cells and this indicated additional antiviral mechanisms for HC and CAPE. Further, in silico analysis indicated that HC and CAPE directly target the viral methyltransferases (MTase) of CHIKV and DENV. A high throughput ELISA-based assay that quantifies m7GMP-nsP1 adduct was employed to validate inhibition of CHIKV nsP1 MTase and IC_{50} was calculated to be 0.009 µM and 0.08 µM for CAPE and HC respectively. Altogether, the identification of natural small molecules as antivirals opens the door for the development of antiviral therapies for the treatment of CHIKV and DENV infections.

Keywords

Dengue virus, Chikungunya virus, Polyamine depletion, Antiviral assay, virtual screening and MD simulation

Introduction

DENV and CHIKV are arthropod-borne viruses belonging to the *Flaviviridae* and *Togaviridae* families, respectively [1]. Both viruses cause febrile illnesses showing fever, arthralgia, joint pain, rash, and headache. These are enveloped viruses having a positive-sense single-stranded RNA genome (+ssRNA) [2]. It is estimated that ~100-400 million DENV infections occur every year [3][4]. Further, in 2021, ~ 0.3 million CHIKV cases occurred worldwide, of which a majority were reported in Brazil and India [5][6]. In India, co-infections with DENV and CHIKV occur prevalently in various regions during the monsoon season [8][9]. [5].

Advances in the understanding of the reliance of viruses on host cell pathways have rekindled interest in targeting the host metabolic pathways for antiviral therapeutics. Viral genomes lack their own protein synthesis machinery, and the ability to hijack the host cell's resources for their own replication is crucial for all viruses. Viruses use various strategies for replication by controlling the host cell's metabolic activities, including exploiting the host lipid pathway, targeting the host glycolytic pathway, hijacking the host ubiquitination pathways, and using the polyamine metabolic pathway [9]. Hence, targeting host factors responsible for virus propagation can be used for the development of broad-spectrum antivirals.

Polyamines are essential molecules in the viral life cycle [12][13]. They are small organic molecules with multiple ionizable amino moieties and are present in all prokaryotes and eukaryotes. A typical polyamine content is indispensable for cell survival and is involved in a wide variety of essential cellular functions. There are three biogenic polyamines in mammals, namely, putrescine (put), spermine (spm), and spermidine (spd), which are produced from ornithine according to the biosynthetic pathway [14][15]. *In vivo*, the enzymatic cleavage of arginine by arginase produces ornithine. Ornithine is converted into putrescine, the first biosynthetic polyamine, by the enzyme ornithine decarboxylase. There is enough evidence to suggest that polyamines are essential for various stages of the virus life cycle, including genome replication, virus protein translation, and genome packaging. Ornithine decarboxylase (ODC) inhibition results in polyamine depletion, which has been shown to depict antiviral

activity against CHIKV, DENV, ZIKA virus (ZIKV), etc. [12][13]. Difluoromethylornithine (DFMO) is a well-known irreversible ODC inhibitor, but it is associated with hearing loss, may suffer antiviral resistance, and requires higher concentrations to show antiviral activity [14]. Hence, an ODC inhibitor with antiviral activity at lower concentrations with less toxicity would be valuable for the development of broad-spectrum highly effective antiviral agents. Natural therapeutic molecules are expected to have low toxicity. Thus, understanding the link between the polyamine biosynthetic pathway and the replication of DENV and CHIKV in infected cells suggests a potential mechanism for antiviral therapies.

Alphaviruses contain four non-structural proteins (nsPs), namely nsP1, nsP2, nsP3, and nsP4, which play an essential role in the life cycle of the viruses and are produced when a viral protease, i.e., nsP2, cleaves the viral polyprotein precursor post-translationally [15]. The capping of viral RNA, performed by nsP1, is a crucial step in the life cycle of an alphavirus. This is because the viral genome cap structure has numerous biological roles, such as helping the eukaryotic translational initiation factor 4E (eIF4e) recognize the RNA for initiating translation and protecting the mRNA from cellular exonucleases [16]. Further, the cap structure also helps the viral genome escape recognition from the host innate immune system pathways such as retinoic acid-inducible gene I (RIG-I) and melanoma differentiation-associated protein 5 (MDA5) [17]. Cellular enzyme capping mechanisms usually involve the methylation of Guanosine triphosphate (GTP) after it has been transferred to the 5’ end of the RNA. However, the molecular mechanism of viral mRNA capping in alphaviruses is distinct. The capping is performed by the Alphaviral capping enzyme, nsP1, in two significant steps. First, S-adenosyl methionine (SAM) acts as a methyl donor to methylate GTP by transferring a methyl group to the seventh position to form m7GMP, where S-adenosyl homocysteine (SAH) is generated as a by-product. This is known as the methyltransferase (MTase) step of the capping reaction [18]. Subsequently, the methylated m7GMP is covalently attached to the nsP1 enzyme via a single bond with His37 during the second step, known as the guanylation (GT) step. In addition, to treat these infections few antivirals targeting alphavirus nsP1 have been identified [19].

Recently, the availability of three-dimensional protein structures of alphavirus nsP1 (6Z0U) has increased the utility of high-throughput computational screening of small molecules in identifying novel drug candidates [20] This strategy exemplifies a logical progression for potential drug discovery against the nsP1 alphavirus.

On the other hand, flaviviruses contain a single open reading frame, which encodes a polyprotein processed by viral and cellular proteases into three structural and seven non-structural proteins (NS1 NS2A, NS2B, NS3, NS4A, NS4B, and NS5). The flavivirus's plus-stranded RNA genome contains a 5’ terminal cap 1 structure (m7GpppAmG). It consists of an N-terminal MTase and a C-terminal RNA-dependent-RNA polymerase (RdRp) domain [21]. The structure of DENV-2 MTase suggests that flavivirus NS5 MTase belongs to a family of SAM-dependent MTases [22].

HC is a naturally occurring flavonoid compound that has multiple pharmacological uses. It is also an established ODC inhibitor that helps lower the levels of polyamines in cells [23]. Further, it has been shown that flavonoids play a role in reducing the levels of nsP1 in CHIKV, and the antiviral activity of flavonoids against CHIKV has been established via various assays, including cytotoxicity assays in Vero cells [24]. CAPE is a natural ester of caffeic acid. Various pharmacological activities such as antiviral, anti-oxidative, and inhibition of human catechol-O-methyltransferase have been reported for CAPE [25][26]. Additionally, CAPE is also a known ODC inhibitor like Herbacetin, which helps reduce the levels of polyamines in cells [27]. Interestingly, the prevailing data shows that polyamines are essential for the replication of a diverse group of viruses[10], [11].

The above-mentioned findings open up new research avenues for exploiting the potential of HC and CAPE as antiviral agents that reduce polyamines level and possibly target virus-specific enzymes. This study has exhibited the fact that both HC and CAPE were able to significantly reduce the virus titer of CHIKV and DENV. Moreover, the compounds have a

dual impact on viral replication as they deplete the polyamine levels in the cells, and also inhibit the viral MTases essential for the capping of viral RNAs.

Materials and methods

Cell line, Virus isolation, propagation and serotyping

Vero cell line was isolated from kidney epithelial cells of an African green monkey, obtained from the National Centre for Cell Science (NCCS), Pune, India. Vero cells were used for the propagation and titration of DENV and CHIKV. The cells were maintained in Dulbecco's Modified Eagles Medium (DMEM) (Gibco, HiMedia) supplemented with 10% inactivated fetal bovine serum (FBS) (Gibco, HiMedia) along with 100 U/mL penicillin and 100 mg/mL streptomycin (Gibco, HiMedia). The cells were maintained at 37°C with 5% CO_2 supplementation.

Dengue was isolated from the DENV-suspected patient's blood samples. Sera was aliquoted and tested for the presence of DENV NS1 antigen by J Mitra ELISA kit according to the manufacturer's instructions. DENV positive samples were used for virus isolation. Initially, sera were 1:10 diluted in minimum essential medium (MEM) (Gibco, HiMedia) containing 2 % FBS, 100 U/mL penicillin, and 100 mg/mL streptomycin for virus propagation. Then, Serum samples were added to a cultivated monolayer of Vero cells for 90 minutes with gentle shaking every 15 min in a 37°C CO_2 incubator. The inoculum was withdrawn, and the cells were cultured for 5-6 days in fresh MEM with 2% FBS and antibiotics until the appearance of cytopathic effect (CPE). After 5-6 days, the supernatant was harvested and serially diluted for infection of Vero monolayer cells for 90 min and overlaid with MEM containing 1 % agarose for the plaque purification procedure. Single plaques were picked and resuspended in MEM and were further propagated in Vero cells. Then DENV NS1 positive supernatants showing CPE was collected and used for further study.

To confirm the DENV and its serotype, RNA from the supernatant of cell culture infected with the virus was isolated using the Trizol (Sigma) method described by the manufacturer. The RNA was then reverse-transcribed into complementary DNA (cDNA) using the PrimeScript cDNA Synthesis Kit (Takara). Synthesized cDNA was utilized as a template for polymerase chain reaction (PCR) [28] and the amplification product was analyzed by gel electrophoresis

in 1 % agarose gels stained with ethidium bromide. The sample was sent for DNA sequencing and the serotype of DENV was confirmed by matching the obtained sequence against the nucleotide database.

CHIKV (GenBank Id: EU372006, strain: DRDE-07) was propagated and titrated in a Vero cell line using the protocol reported by Singh et al., 2018 [31], [32] and then stored at −80 °C for further experiments.

Preparation of HC, CAPE, and DFMO stock solutions

HC, CAPE, and DFMO were purchased from Cayman, USA. For experiments, the stock solutions (HC: 165.45mM; CAPE: 20mM) for both compounds were prepared in dimethyl sulfoxide (DMSO) (Sigma- Aldrich) and filtered through a 0.2µm size syringe filter (Millipore). The 100mM DFMO dilution was prepared in sterile tissue culture grade water, i.e., used as a positive control for the polyamine-related experiments. At the time of usage, further dilutions were prepared in culture media. Similarly, individual polyamines (put, spm, and spd) (Alfa-Aeser, USA) stocks were diluted in water and used as designated.

Polyamine determination by Thin-layer chromatography (TLC)

Polyamines were separated by TLC as previously described [31]. For all samples, cells were treated as described before being trypsinized and centrifuged. Wash with PBS. Sonicate the cells in 500 µL of 2% (V/V) perchloric acid. Sonication was performed at 4ºC (20 kHz, 2Ω, 10-sec pulse, 30-sec rest). Cell homogenates obtained are then stored at 4ºC for 24 hrs. After 24 h, samples are centrifuged at ~11,500 g for 30 min at 4ºC. An equal ratio of supernatant dansyl chloride (5 mg/ml) (Alfa-Aesar, USA) was added in acetone and saturated sodium bicarbonate. Samples were incubated in the dark overnight at room temperature. Excess dansyl chloride was cleared by incubating the reaction with 150 mg/mL proline (HiMedia). Dansylated polyamines were extracted with 100 µL toluene. 10 µL of the sample was added in small spots to the TLC plate by automated sprayer (Silica gel matrix; Millipore) and exposed

to ascending chromatography with cyclohexane:ethyl acetate (2:3). The plate was dried and visualized via exposure to UV.

Cell Cytotoxicity Assay

Different concentrations of HC and CAPE were evaluated for cytotoxicity on Vero cells using 3-(4,5-dimethyl-thiazol-2-yl)-2,5-diphenyltetrazolium bromide (MTT) (Himedia) assay. Before treatment, Vero cells were seeded in a 96 well plate and at 90% confluency, the media were removed, and different dilutions of compounds were added into each well for 24 h. After incubation, the inoculum was removed and fresh maintenance media were added for 2 h. Further fresh compound dilutions were added to each well and kept for 24 h. Subsequently, 20 µL/well of MTT (5mg/mL) was added and incubated for 4 h at 37°C in 5% CO_2. Upon incubation, 110 µL/well of DMSO was added to dissolve formazan crystals. Plates were read at a wavelength of 570 nm using citation three multi-mode plate reader (BioTek Instruments, Inc.). The average absorbance of 0.1 % DMSO treated cells was used as cell control. In the second set of experiments, after completion of 24 hrs post-treatment, fresh maintenance media were added and kept for 4 days. The cell viability of the treated well was compared with the cell control, and the concentration which showed >90% viability after compound treatment was considered non-toxic. The experiment was performed in triplicates.

Assessment of Antiviral Activity

Vero cells were seeded onto a 24-well plate at a cell density of 1.0 x 10^5 cells/well. Cells were treated with compounds 12 h before infection. With a multiplicity of infection (MOI) of 0.1, the cell monolayer was infected with the virus with gentle shaking every 15 minutes for 2 hrs. The inoculum was removed, and the cell monolayer was washed twice to ensure no chance of secondary infection. Compounds were also added in the post-infection (pi) 2% DMEM media and incubated for 24 h. After 24 hpi, the supernatant was collected for CHIKV antiviral experiment. On the other hand, fresh maintenance media was added in the DENV antiviral

experiment for 4 days. Then, the supernatant was collected for determining virus titre via plaque-forming assay.

Polyamine addition to rescue virus

In polyamine addition assay, drug pre-treatment was given for 24 h at various concentrations such as HC (200 µM), CAPE (25 µM for CHIKV and 2.5 µM for DENV), DFMO (1000 µM). After infection with CHIKV and DENV, cells were treated with 1 µM biogenic polyamines (put, spd, spm) for 24h and 120 h respectively. Later, the supernatant was collected for determining virus titer by plaque-forming assay.

Plaque Reduction Assay

Vero cells were seeded at 1.0 x 10^5 cells/well in a 24-well plate in complete media before infection. The supernatant was 10-fold serially diluted in maintenance media and was inoculated on ~80-90% confluent cells. Plates were incubated for 2 h with a gentle shaking every 15 min for virus adsorption at 37°C with a 5% CO_2 incubator. After adsorption, overlay media and maintenance media in 1:1 dilution and plates were further incubated for 2 days and 3 days for CHIKV and DENV respectively at 37˚C in 5% CO_2 incubator. Following that, cells were stained with 1% crystal violet to count the number of CHIKV plaques and immunostaining for DENV-infected cells, as described below.

Immunostaining was performed at room temperature. After incubation, overlay media was removed from the plates, and the cell monolayer was fixed with 3.7% formaldehyde solution for 30 min. Cells were washed 3 times with PBST (0.02% Tween-20 in Phosphate buffer saline). After that, cells were permeabilized with 0.2% triton X-100 in PBS for 7 min. Cells were washed three times with PBST and incubated with 3% Skim milk for 30 min. Then, cells were washed three times with PBST and incubated with 1:500 diluted flavivirus group antibody (Genetex) for 2 h. Cells were washed three times with PBST and incubated with secondary antibody (Goat anti-mouse IgG HRP, 1:1500 dilution) for 1 h. After washing 2 times with PBST and three times with PBS, cells were stained with True Blue Peroxidase substrate (KPL,

Sera Care, MA, USA) and incubated in the dark for 30 min to develop blue colour staining of virus-infected cells and foci were counted [29].

Immunofluorescence Assay

Vero cells were seeded onto a 6-well plate at a cell density of 1 x 10^6 cells/ well. Cells were treated with compounds as mentioned earlier. The cells were washed three times with PBS and then fixed with methanol:acetone (1:1) for 1 h at room temperature followed by permeabilization with 0.1% Triton-X-100. After washing, cells were incubated with antibodies against CHIKV and DENV (anti-alphavirus 1:100, SANTA Cruz Biotechnology Inc, 1:500 diluted flavivirus group antibody (Genetex Inc).) for 1 h and then incubated with fluorescein (FITC)-conjugated secondary anti-mouse antibody (1:250, Sigma) for 30 min at 37 °C. The plate was then rinsed with PBS and counter-stained with 4′,6- diamidino-2-phenylindole DAPI (Sigma) for 15 min. Then, the image was captured under a fluorescence microscope (EVOS, Thermofisher). All experiments were repeated thrice to verify the results.

Quantitative Real-Time PCR (qRT-PCR)

Vero cells were seeded into 6 well plates prior the day of infection. HC and CAPE compounds treatment and infection were the same as described in the assessment of antiviral activity. After the termination of an assay, trizol was added to the plate. RNA was purified according to the manufacturer's protocol. Purified RNA was quantified and used for cDNA preparation using the PrimeScript 1st strand cDNA Synthesis Kit (Takara) with 1 µg of extracted RNA. The forward and reverse primers used for amplification are used as previously described in [28] and [30]. qRT-PCR was used to determine the effect of HC and CAPE on CHIKV and DENV replication by counting the number of copies of RNA. All experiments were carried out three times in triplicates.

Multiple Sequence Alignment (MSA)

The amino acid sequence of different alphaviruses nsP1 protein was compared with CHIKV nsP1 as a reference point using Clustal Omega [32] to check if the key residues involved in the

capping of viral RNA were conserved across different viruses. The MSA was performed for Venezuelan equine encephalitis virus (VEEV) (AWT57896), CHIKV (AWQ38330), Ross River virus (RRV) (AAU89533), Sindbis virus (SINV) (ABL84688), Aura Virus (AURA) (QVM79755), Middelburg virus (MIDV) (QOW97289), Barmah Forest virus (BFV) (QOY44469), Madariaga virus (MADV) (QTC33397), and Mayaro virus (MAYV) (AZM66145) from the Alphavirus family. The sequence alignment profile of the selected nsP1 sequences was performed via Clustal Omega tool and analyzed by a graphical colored depiction using ESPript 3.0 [37].

Similarly, multiple sequence alignment was performed for the MTase domain of NS5 from Dengue 3 Virus (DENV 3) (4CTJ_1), Zika Virus (ZIKV) (5WZ2_1), West Nile Virus (WNV) (2OY0_1), Yellow Fever Virus (YFV) (3EVA_1), and Japanese Encephalitis Virus (JEV) (4K6M_1) from the flavivirus family. And the analysis was carried out in the same way as for DENV.

Molecular Docking of HP and CAPE into MTases

The cryo-electron microscopy (cryo-EM) structure of CHIKV nsP1 has been published at 2.6 Å and 2.9 Å resolution (6Z0V, 6Z0U, and 7DOP) [20]The structure reveals the catalytic binding site in nsP1, where SAM and GTP bind during RNA capping [33][34]. The protein data bank (PDB) entry lacked atomic coordinates for multiple flexible loops; therefore, SWISS Model [35] was utilized to create a model of nsP1 using 6Z0U as a template and 6Z0V as the sequence prior to docking. AutoDock Vina software algorithm [36] was utilized in all the docking and simulation experiments, with the optimized model as the target. The structures of HC, CAPE, GTP, and SAM, as ligands were obtained from the PubChem site in .sdf format and then converted to. pdbqt format using OpenBabel in PyRx 0.8 algorithm [37], [38]. In AutoDock Vina, centre grid dimensions were specified as 29.50 Å × 23.35 Å × 27.91 Å, centered at X = 56.15, Y = 135.85, and Z = 88.22, for the CHIKV nsP1.

Similarly, the 3D structure of DENV NS5 MTase (PDB ID 4V0R) was obtained from PDB[39] Furthermore, the literature reveals the SAM or SAH binding site to be Asp79, Leu80, Gly81, Cys82, Gly83, Arg84, Gly85, Trp87, His110, Asp131, and Phe133 [40]. The centre grid dimensions were specified as 17.95 Å × 24.98 Å × 17.13 Å, centered at X = 27.91, Y = 127.90, and Z = 20.88, located at the active site of NS5 MTase. The conformations with the best binding energy were further analyzed in PyMol and LigPlot^{+} software [41], [42].

Molecular Dynamics (MD) Simulations

nsP1 and ligands were subjected to MD simulation studies to assess the flexibility and stability of protein-ligand interactions. The same study was carried out for DENV NS5 MTase with SAM, HC, and CAPE. For this purpose, GROMACS 5.4.1 suite was used to carry out all simulation studies using the GROMOS96 43a1 force field on a LINUX-based workstation [43]. Ligand parameters and topology files were generated using the PRODRG server [44]. Furthermore, ions and water molecules were added to neutralize the whole cubic system for solvation. The energy minimization step was performed using the steepest descent method, followed by a two-phased equilibration of a constant number of particles, volume, and temperature (NVT), a constant number of particles, pressure, and temperature (NPT). NVT equilibration was done at 300K with a short-range electrostatic cut-off of 1.2 nm, and temperature regulation was done using the Berendsen temperature coupling method. Further, the next phase of equilibration NPT was performed, and coordinates were generated every 1 ps. Finally, 50 ns MD production run was performed with an integration time frame of 2fs, and the trajectories were generated after every 10 ps. The conformations generated during the production step were used for calculating root mean square deviation (RMSD) of protein-ligand complexes

CHIKV nsP1 enzyme inhibition assay

CHIKV nsP1 protein was purified using the same protocol as reported earlier [45][19][46]. To test nsP1 inhibition by HC and CAPE, nsP1 enzyme reaction was performed in a reaction

mixture consisting of 50 mM Tris buffer (pH 7.3), 10 mM NaCl, 5 mM DTT, 2 mM $MgCl_2$, 100 μM SAM and 100 μM GTP along with 20 μM protein at 25 °C for 30 min. Different concentrations of CAPE (1 μM, 5 μM, 25 μM, 50 μM, 150 μM, and 300 μM) and HC (25 μM, 50 μM, 100 μM, 150 μM and 300 μM) was used for the inhibition assay. CHIKV nsP1-m7GMP conjugate formation activity of purified nsP1 was detected with the help of ELISA-based nsP1 assay using the same protocol reported earlier [19].

Statistical analysis

GraphPad Prism was used to determine IC_{50} values using a sigmoidal dose–response (variable slope) equation. One-way ANOVA was used to determine statistical significance in comparisons of positive control and compound cytotoxicity and antiviral activity measures, followed by Dunnett's tests. When $p < 0.05$, a difference was considered significant.

Results

Antiviral and polyamine depletion activities of HC and CAPE

For this study, DENV serotype was isolated from a clinical sample and DENV3 serotype (Accession No. OM921607) was confirmed by PCR using virus and serotype-specific primer pairs and sequencing.. The basic local alignment search tool (BLAST) tool revealed 99.78% identity of isolated DENV serotype to DENV3 isolate NU1883 polyprotein (POLY) gene, partial cds. Similarly, CHIKV (Accession No. KY057363.1.) was propagated in vero cells and used in the further study The MTT colorimetric assay was performed for testing the cytotoxicity of HC and CAPE. The cell viability of >90% was observed for HC upto 200 µM and CAPE upto 25 µM (Figure 1A-C). Antiviral activities of HC and CAPE at various concentrations were determined against CHIKV in plaque reduction assays performed in Vero cells using the maximum non-cytotoxic concentrations (MNCC) of each compound. By comparing the viral titre of untreated CHIKV infected cells with HC and CAPE treated CHIKVs infected cells, a dose-dependent decrease in CHIKV titre was observed for both the compounds (Figure 1 D-E). DFMO, a known ODC inhibitor was used as a control and it showed less antiviral efficacy against CHIKV at much higher concentrations of 1000µM as compared to HC and CAPE. HC and CAPE effectively inhibited CHIKV with EC_{50} values 463 nM and 0.417 nM respectively. Similarly, a dose-dependent inhibitory effect of HC and CAPE was observed for DENV-3 with EC_{50} values 8.5 µM and 1.15 µM, respectively. DFMO used a positive control and showed antiviral activity against DENV which was comparable to HC and CAPE (Figure 1 G-H).

Conventional RT-PCR methods are still reliable diagnostic methods for studying viral load in supernatants and clinical samples. Here, qRT-PCR was used for validating the antiviral effect of HC and CAPE by quantifying DENV and CHIKV RNA levels in the infected cells. qRT-PCR showed a significant ($p < 0.0001$) reduction in the viral RNA levels when treated with HC and CAPE compounds in an antiviral assay for CHIKV (Figure 1F) and DENV (Figure 1I)

At the mentioned concentrations, HC and CAPE showed a 23- and 4-fold reduction in DENV, respectively, compared to the VC. Similarly, at the same doses, HC and CAPE reduced CHIKV by 25 and 97 times, respectively, compared to VC. These results were further corroborated with IFA results. The results of IFA analysis showed a reduction in CHIKV (Figure 2 A) and DENV (Figure 2 B) virus after treatment with HC and CAPE.

Further, TCL experiments were performed to determine the effect of HC and CAPE on polyamine levels in mammalian cells treated with these compound. Vero cells were treated with HC, CAPE and DFMO and TLC results confirmed a reduction in the levels of all three polyamines. Polyamine levels in cells treated with CAPE were significantly lower as compared to DFMO treatment (Figure 1J). Whereas, HC showed a reduction in polyamine levels with initially 12 hrs treatment but later levels of polyamine elevated with time. Overall, CAPE and HC showed higher polyamine depletion at lower concentrations as compared to the positive control (DFMO) and the cell control (Figure 1J).

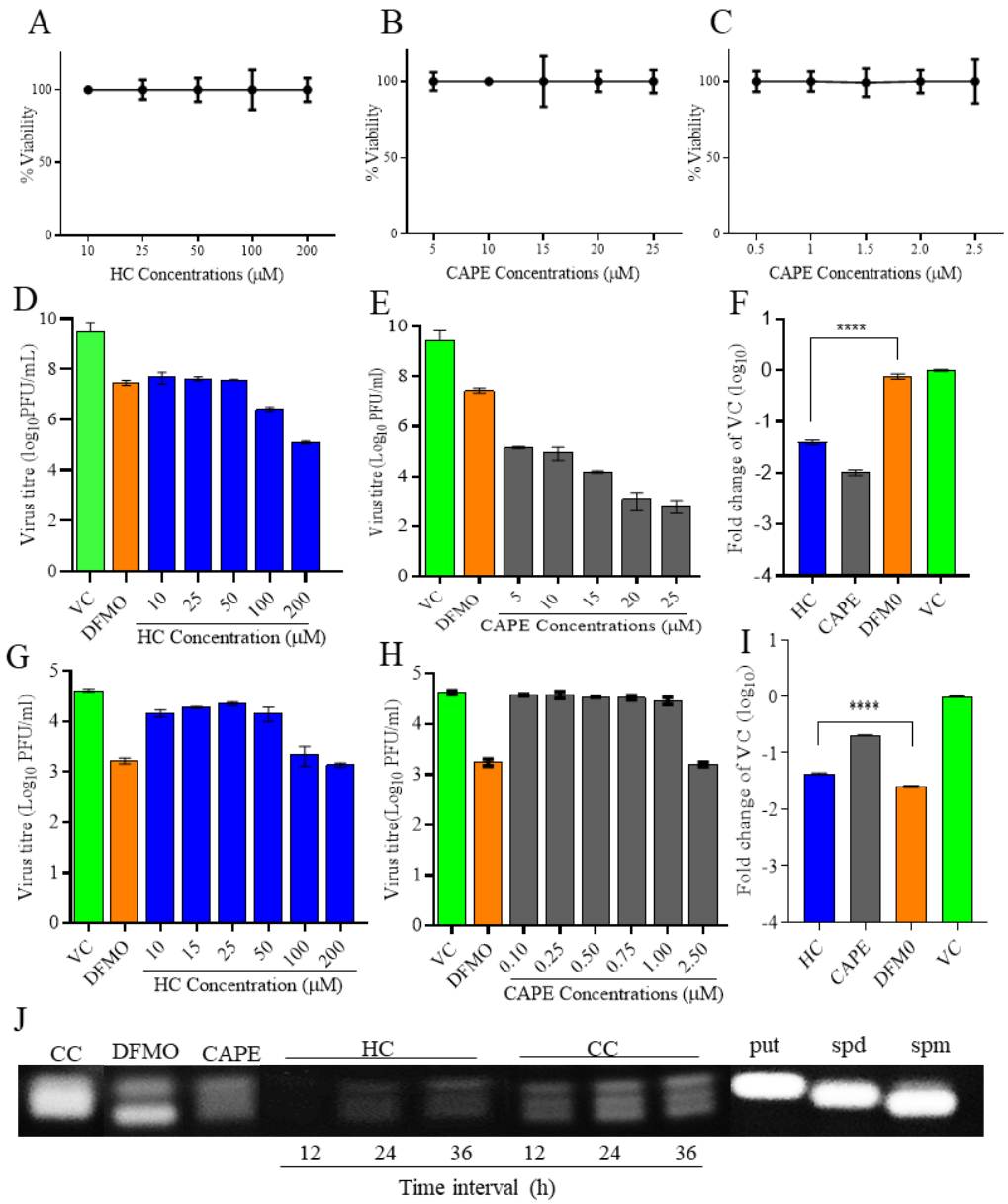

***Figure 1**: Evaluation of antiviral activity using virus titer reduction profiling of HC and CAPE. Panel A-C depicts the percent cell viability of Vero cells treated with HC and CAPE for 12 h pre-treatment and 24 h post-treatment for 4 days, Panel B showing the percent cell viability of Vero cells treated with CAPE for 12 pre-treatment and 24 h post-treatment. Cell viability for all tested concentrations remained above the cytotoxic threshold of 90%. Panels D-G depicts the inhibitory effect of CHIKV and DENV infected cells on different concentrations of HC and CAPE. Vero cells were infected with CHIKV (D-F) and DENV (G-I), with DFMO (1000 µM) serving as a positive control and VC representing virus control. Panel J depicts the effect of polyamines level after treating with HC (200 µM) and CAPE (25 µM). Polyamine level of Vero treated cells at 12, 24, and 36 h for HC and pre (12 h) and post-treatment (24 h) for CAPE and DEMO, using untreated cells as a cell control (CC) for both of the conditions. 0.1 µM putrescine (put), spermine (spm), and spermidine (spd) as a positive control marker. Treatment with both compounds leads to decreased polyamine levels for both of the compounds compared to*

*DFMO. Error bars represent the standard error of experimental replicates with n = 3. Statistical analysis was performed using one-way ANOVA with Dunnett's post-test. ***P < 0.001.*

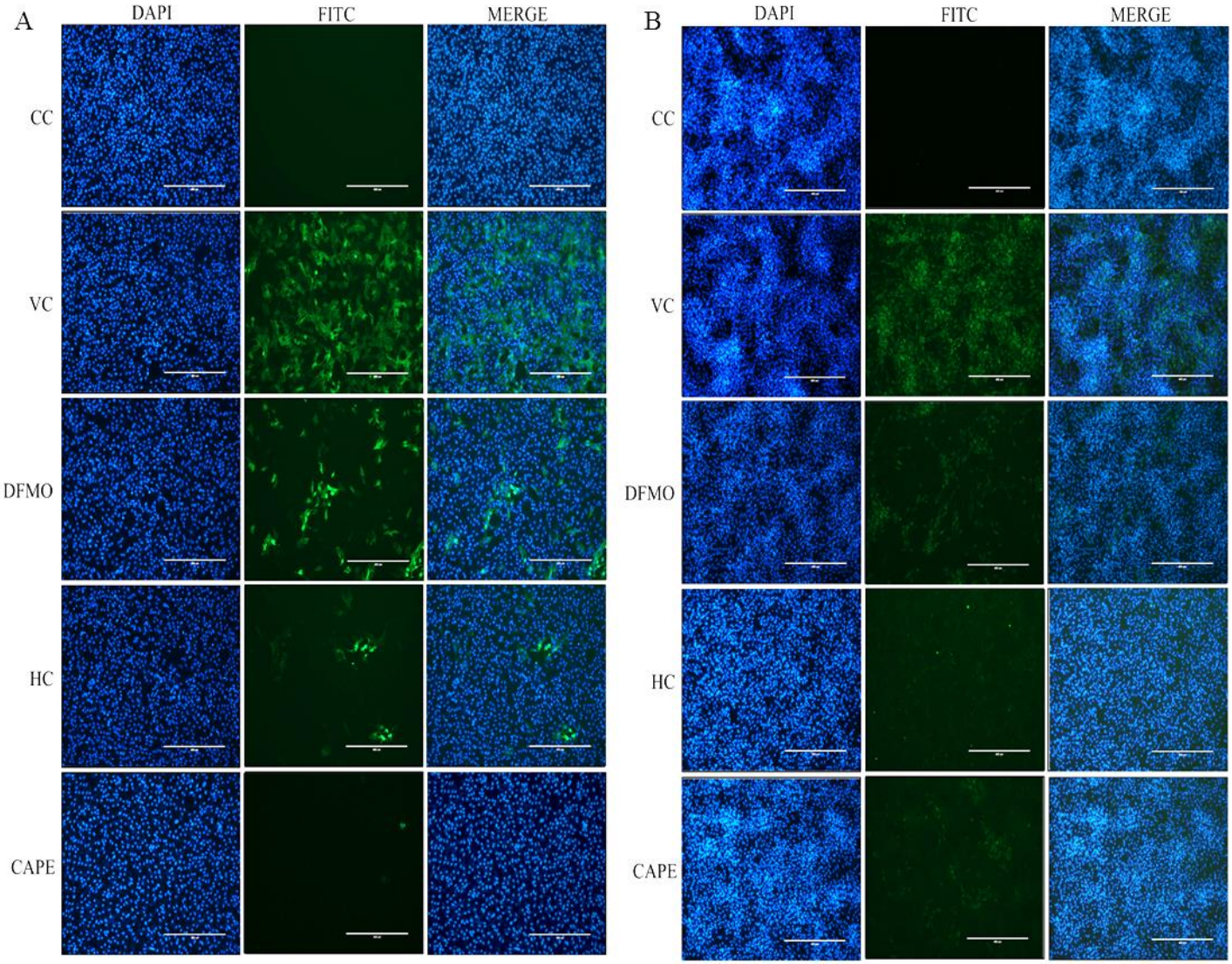

Figure 2: *Evaluation of the antiviral effect by immunofluorescence assay (IFA). Immunofluorescent staining of HC (200 µM) and CAPE (25 µM for CHIKV and 2.5 µM for DENV) treated with CHIKV(A) and DENV(B) in Vero cells. Green fluorescence (FITC) indicates the virus load, and blue fluorescence (DAPI) indicates the nuclear staining with DAPI with a 10× objective lens. The scale bar is 400 µM. DAPI: 4',6-diamidino-2-phenylindole; FITC: Fluorescein isothiocyanate; CC: Cell Control; VC: Virus Control.*

Further, the effects of the addition of exogenous biogenic polyamines were studied. Vero cells were pre-treated with drugs at various concentrations such as HC (200 µM), CAPE (25 µM for CHIKV and 2.5 µM for DENV), and DFMO (1000 µM). After infection, 1 µM each of

exogenous polyamines (put, spd, spm) were added. Unlike DFMO treated cells, externally addition of all three polyamines at 1 µM were unable to effectively rescue virus titre after CAPE and HC treatment for both CHIKV and DENV (Figure 3). Hence, this observation indicates that CAPE and HC may have other mechanisms that play a role in the antiviral activity of these compounds against both viruses.

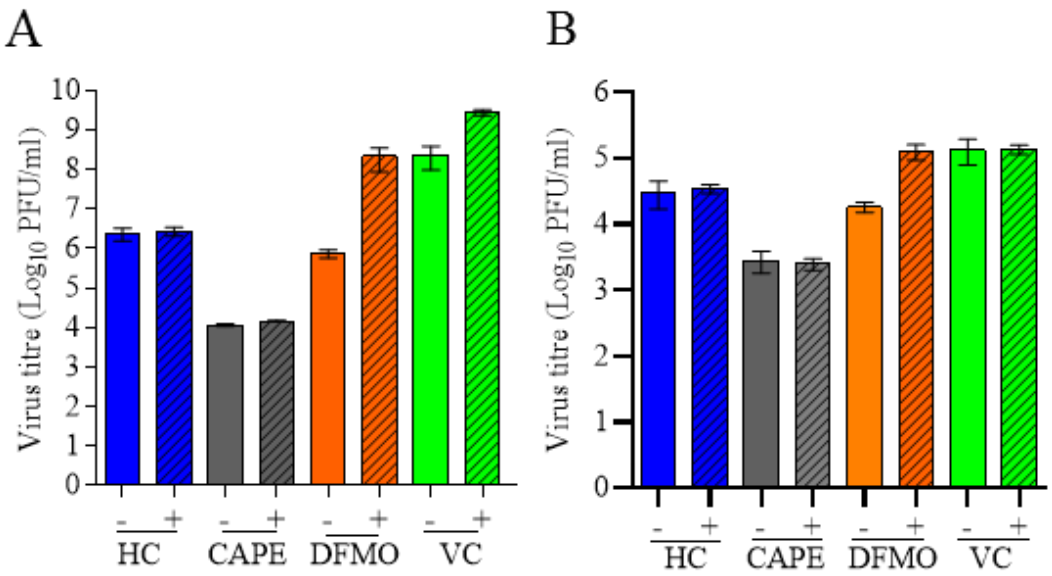

Figure 3: *Effect of addition of biogenic polyamines on virus infected and drug-treated cells. Vero cells infected with CHIKV (A) and DENV (B) treated with HC (200 µM), CAPE (25 µM for CHIKV and 2.5 µM for DENV), DFMO (1000 µM) as a positive control and VC (Virus Control) as untreated control. – (minus) sign indicates only the drug treated Vero cells whereas + (plus) sign indicates that 1uM polyamines (put, spd, spm) was added additionally in the drug treated cells. Error bars represent the standard error of experimental replicates with n = 3.*

CAPE, a natural ester of caffeic acid is a known effective inhibitor of catechol-O-methyltransferase [27, 28]. Additionally, it has been reported that flavonoids are potential antiviral agents that inhibit CHIKV replication [26], and HC is a naturally occurring flavonoid compound that has multiple pharmacological uses. Hence, the possibility of HC and CAPE binding and targeting virus-specific MTases i.e. nsP1 of CHIKV and NS5 of DENV were further examined.

SAM-dependent methyltransferases as direct-antiviral targets of HC and CAPE:

The availability of recently determined cryo-EM atomic structure of CHIKV nsP1 capping enzyme containing virus-specific MTase enzyme activity and the crystal structure of DENV NS5 MTase (PDB ID 4V0R) facilitated *in silico* structure-based analysis of HC and CAPE as potential MTase inhibitors [22, 43]. GTP-binding site is formed by residues Ala40, Arg41, Ser44, His45, Lys49, Arg70, Arg71, Gln151, Asp152, Tyr154, Tyr248, Tyr285 in CHIKV nsP1. Additioanlly in CHIKV nsP1, the SAM-binding residues are well-defined by residues common to the GTP-binding site (Arg70, Arg71, Gln151 and Asp152) and others unique residues for the binding of SAM in nsP1 are Gly65, Pro83, Glu88, Asp89, Arg92, and Val153 [20]. Structural analysis of DENV NS5 MTase has revealed that the SAM binding site residues for flaviviruses are Asp79, Leu80, Gly81, Cys82, Gly83, Arg84, Gly85, Trp87, His11 0, Asp131, and Phe133 [43, 44]. Primary sequence alignment and comparison of various members of the alphaviruses and flaviviruses revealed high sequence similarity as shown in Figure 4A. In alphaviruses, 94.4% of the active site residues showed 100% sequence identity across nsP1 of different viruses. Whereas, in flaviviruses, 90.9% of the active site residues showed 100% sequence identity across NS5 MTase when compared (Figure 4B). The MTase active site residues that are sequentially, structurally and functionally conserved in nsP1 and NS5 are potential drug target sites and were in silico examined for binding to the HC and CAPE molecules.

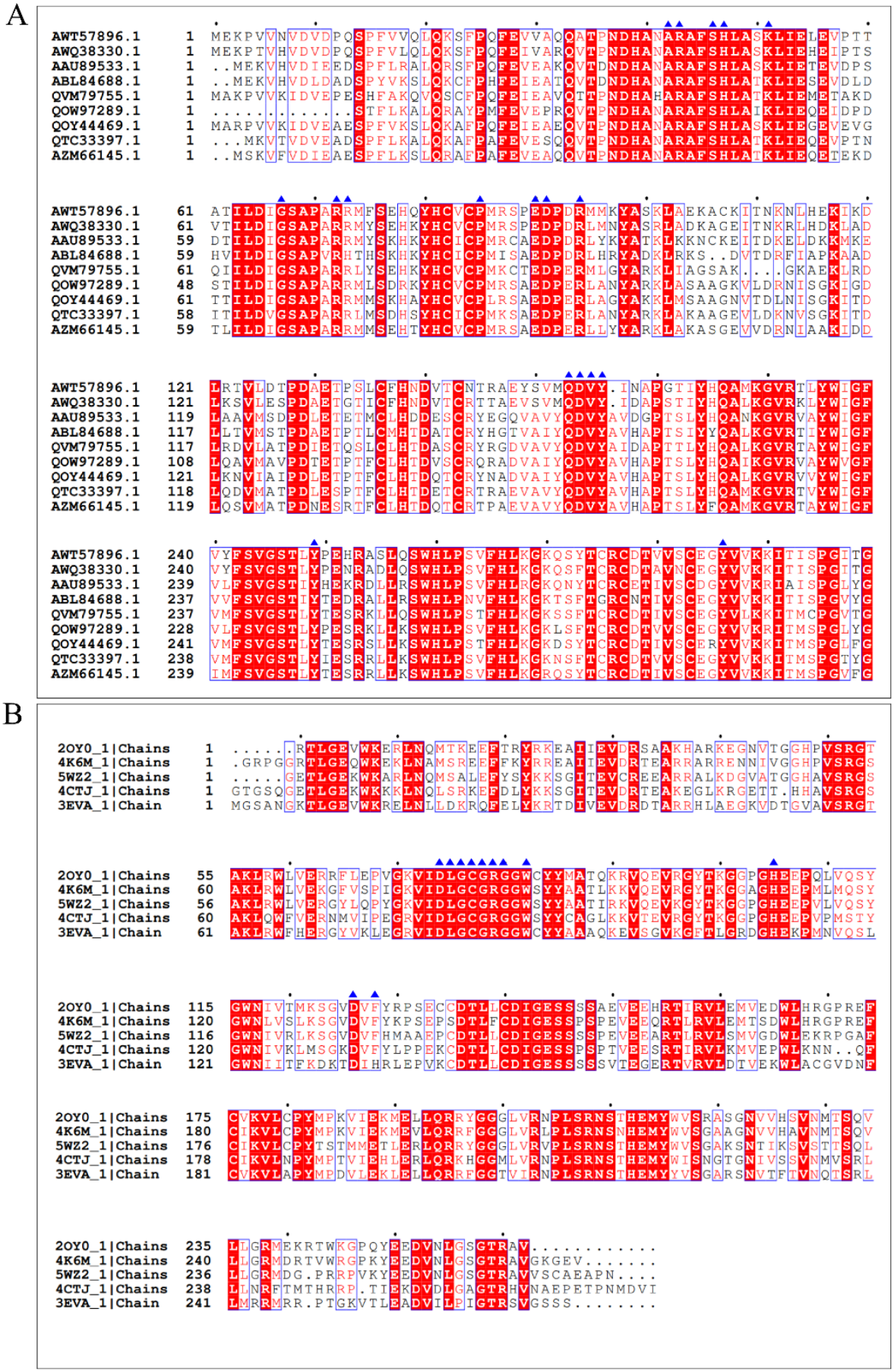

Figure 4: *Multiple Sequence alignment of MTase domains of different alphaviruses and flaviviruses. A) Sequence alignment of nsP1 MTase domain from CHIKV with the MTase domains of other alphaviruses. B) Sequence*

alignment of NS5 MTase domain from DENV with MTase domains of other flaviviruses. The active-site MTase residues in both alphaviruses and flaviviruses are highly conserved suggesting that structure and function of MTase domain in both families are conserved. Residues are represented with single letter amino acid code, with identical residues indicated in white font and boxed in red, while similar residues are indicated in red font. Blue triangles are corresponding to the MTase active site residues as per literature. Alignments were generated via Clustal Omega and ESPript tools. The MSA was performed for Venezuelan equine encephalitis virus: AWT57896; chikungunya virus: AWQ38330; Ross River virus: AAU89533; Sindbis virus: ABL84688; Aura Virus: QVM79755; Middelburg virus: QOW97289; Barmah Forest virus: QOY44469; Madariaga virus: QTC33397; and Mayaro virus: AZM66145) from the Alphavirus family. The multiple sequence alignment was performed for the MTase domain of NS5 from Dengue 3 Virus: 4CTJ_1; Zika Virus: 5WZ2_1; West Nile Virus: 2OY0_1; Yellow Fever Virus: 3EVA_1; and Japanese Encephalitis Virus: 4K6M_1 from the flavivirus family.

For molecular docking of HC and CAPE to evaluate binding of these molecules to the viral MTases, the alphavirus CHIKV nsP1 structure and flavivirus DENV NS5 MTase domain structures were generated using SWISS-MODEL as PDB entry (6Z0U and 4V0R) lacked few atomic coordinates for multiple flexible loops. The generated models were superimposed on to the template of each of the virual protein using PyMOL 2.3 and the RMSD was calculated. The 2D image with the superimposed amino acid residues are highlighted and shown in Supplementary figure 1. Structural comparison of the generated models of CHIKV and DENV with respective templates showed high structural similarity with low RMSD values i.e., 0.205 Å and 0.182 Å respectively (Supplementary figure 1). CHIKV nsP1 and DENV NS5 MTase generated models were further used for flexible docking of HC, CAPE, and the positive controls i.e.; SAM and GTP. The positive control showed binding energy in the range of -7 to -8.2 kcal/mol. Interestingly, the binding affinities of both the compounds obtained were similar or higher than the positive control for both the viruses. It was observed that HC and CAPE form hydrogen (H) bonds with the active site residues of CHIKV nsP1 and make hydrophobic interactions as well (Table 1). While, in DENV NS5 MTase, it was observed that along with the active site residues the H-bonds were also formed with the residues that are in the vicinity of the active site (Table 2). The attained binding energies of HC and CAPE along with the

positive controls and detailed protein-ligand interactions are presented in Table 1-2 and Figures 5-6.

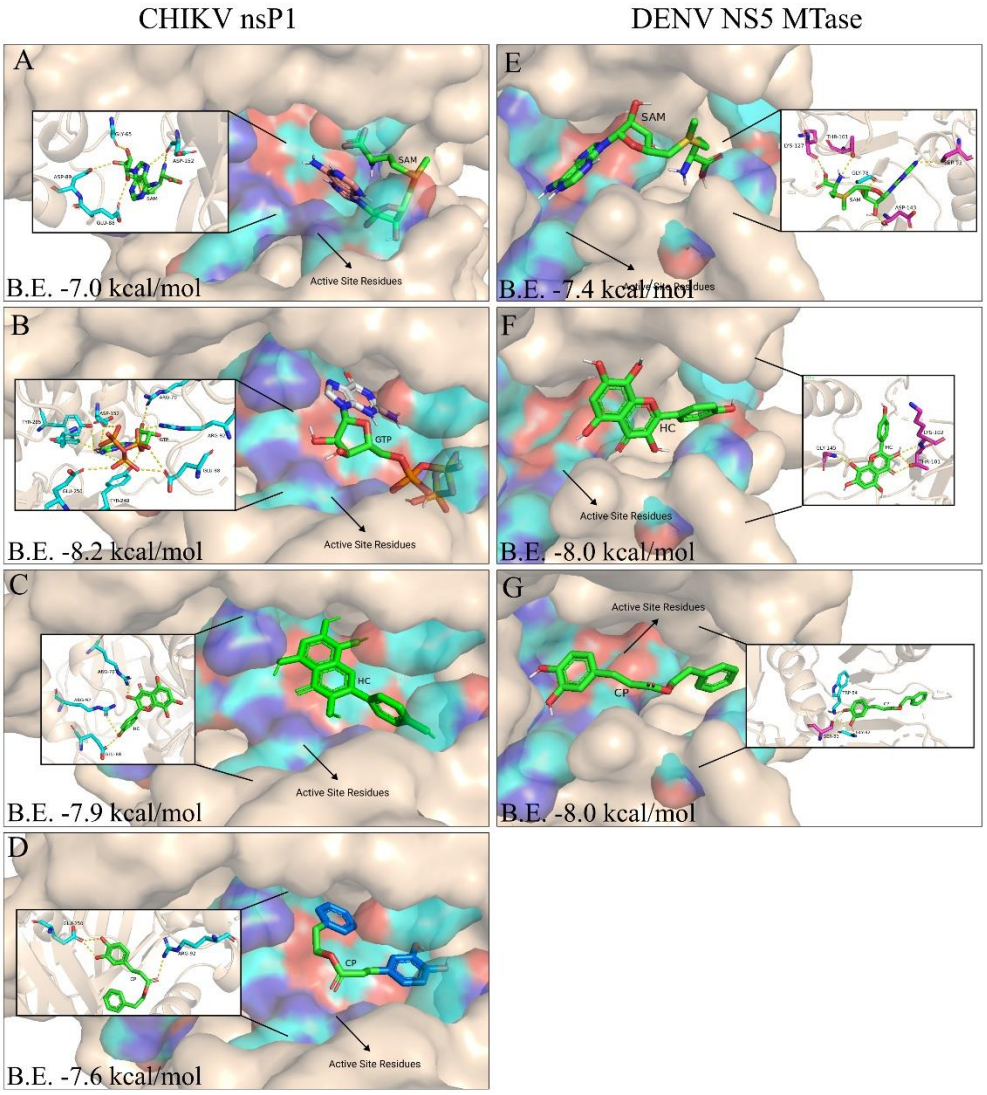

Figure 5: *Ligands docked in the binding site pocket (teal surface) of CHIKV nsP1 and DENV NS5 (wheat surface). A-D) CHIKV nsP1 interact with the SAM (A), GTP (B), HC (C) and CAPE (D); E-G) DENC NS5 MTase interact with SAM (E), HC (F), and CAPE (G). Zoomed in figures show a detailed view of the binding pocket where molecular interactions of ligands (green) with binding active site residues (teal colour) and additional binding residues (pink colour) of CHIKV nsP1 and DENV NS5 MTase (wheat coloured protein ribbon/ surface).*

CHIKV nsP1

DENV NS5 MTase

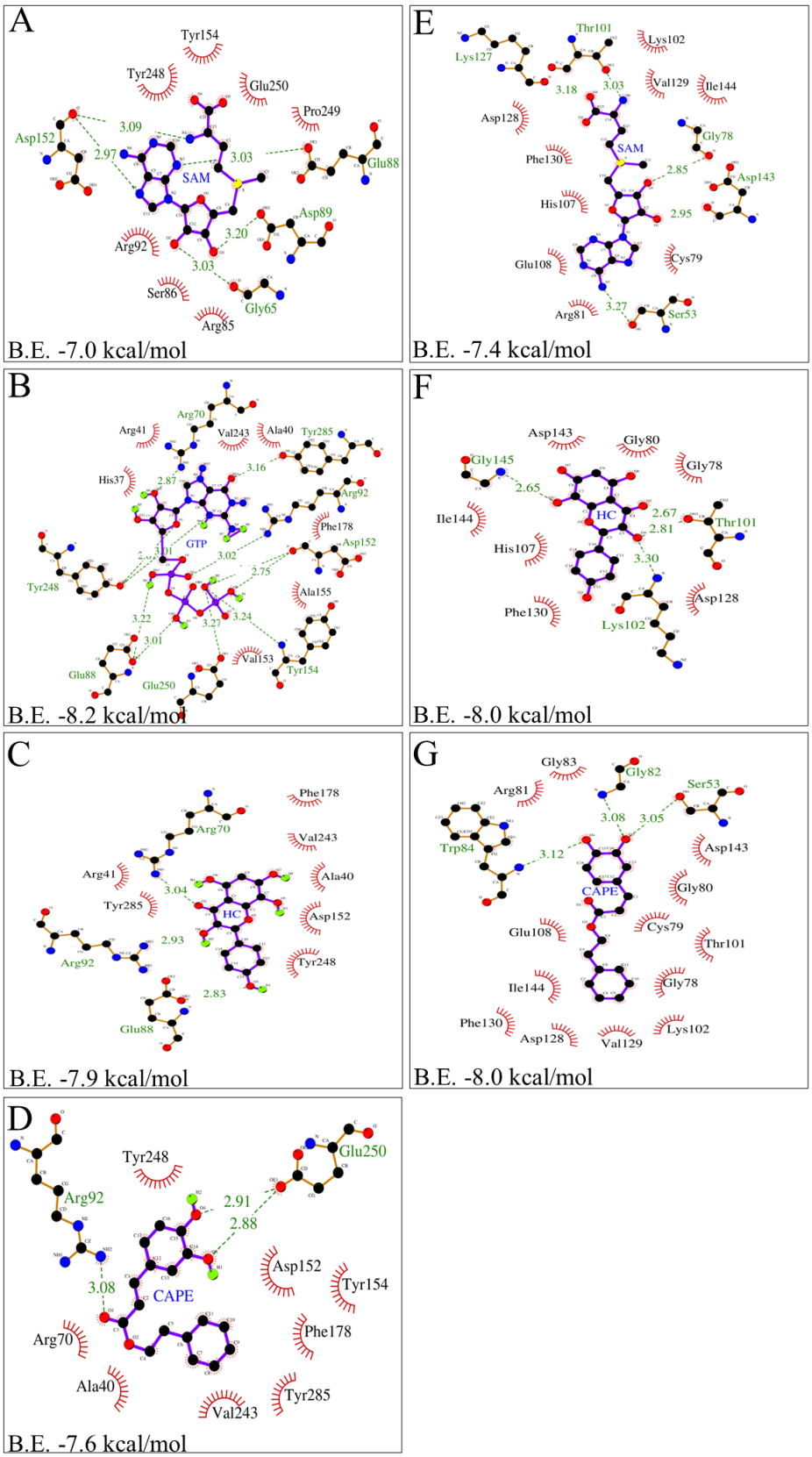

***Figure 6**: Two-dimensional representation view of docked molecules in LigPlot+ software to visualise the interacting residues with the CHIKV nsP1 and DENV NS5 MTase. A-D) CHIKV nsP1 interact with the SAM (A), GTP (B), HC (C) and CAPE (D); E-G) DENC NS5 MTase interact with SAM (E), HC (F), and CAPE (G). H-bonds are shown in green dashed lines with the distance shown in Å. Additional residues forming hydrophobic interactions are shown by brown semicircle with radiating spokes towards the ligands.*

Table 1: Detailed molecular interactions between the CHIKV nsP1 and ligands.

Ligand	Binding energy (kcal/mol)	Interactions			
		Hydrogen			Hydrophobic interactions
		Residues	Molecules	Bond length (Å)	
GTP	-8.2	Glu88	O10- OE1	3.01	His37, Ala40, Arg41, Val153, Ala155, Phe178, Val243
			O11- OE1	3.22	
		Tyr248	N2-OH	3.01	
			O1-OH	2.67	
		Arg70	O14 - NH1	2.87	
		Tyr285	O13-OH	3.16	
		Arg92	O3-NH2	3.02	
		Asp152	H2-O	3.12	
			O8-O	2.75	
		Tyr154	O9-N	3.24	
		Glu250	O9- OE1	3.27	
SAM	-7.0	Asp152	N1-O	3.09	Arg 85, Ser86, Arg92, Tyr154, Tyr248, Pro249, Glu250
			N5-O	2.97	
		Glu88	N3- OE1	3.03	
		Asp89	O3-OD2	3.20	
		Gly65	O2-O	3.03	
HC	-7.9	Glu88	O3-OE1	2.83	Arg41, Tyr285, Phe178, Val243, Ala 40, Asp152, Tyr248
		Arg92	O4-NH2	2.93	
		Arg70	O2-NH1	3.04	

CAPE	-7.6	Arg92	O1-NH2	3.08	Arg70, Tyr248, Asp152, Tyr154, Phe178, Tyr285, Val243, Ala40, Arg70
		Glu250	O4 -OE1	2.91	
			O3-OE1	2.88	

Table 2: Detailed molecular interactions between the DENV NS5 MTase and ligands.

Ligand	**Binding energy (kcal/mol)**	**Interactions**			
		Hydrogen			**Hydrophobic interactions**
		Residues	**Molecules**	**Bond length (Å)**	
SAM	-7.4	Gly78	O-O5	2.85	Lys102, Val129, Asp128, Phe130, Ile144, His107, Glu108, Cys79, Arg 81
		Ser 53	OC-N5	3.27	
		Asp143	O2-O	2.95	
		Thr101	N6-OG1	3.03	
		Lys127	O4-O	3.18	
HC	-8.0	Thr101	OG1-O2	2.67	Asp143, Gly80, Gly78, Ile144, His107, Asp128, Phe130
			OG1-O4	2.81	
		Lys102	N-O4	3.30	
		Gly145	N-O5	2.65	
CAPE	-8.0	Trp84	N-O4	3.12	Gly83, Arg81, Asp143, Gly80, Glu108, Cys79, Thr101, Ile144, Gly78, Phe130, Asp128, Val129, Lys102
		Gly82	N-O3	3.08	
		Ser53	OG-O3	3.05	

The dynamic stability and conformational changes in the apo proteins and protein-ligands complexes were studied by analyzing their RMSD during the MD simulation. RMSD data showed that all the nsP1-ligand complexes attained equilibrium at 15 ns and reached stable state throughout the simulation for up to 50 ns (**Supplementary figure 2A**). Equilibrium was attained after 15 ns and fluctuations were found to be in the range of 0.6 to 0.75 nm for nsP1

Apo and nsP1-GTP, 0.35 to 0.55 ns for nsP1-SAM, nsP1-HC, and nsP1-CAPE. Similar MD simulation based RMSD study performed for DENV NS5 MTase showed the Apo NS5 MTase and the NS5 MTase-SAM complex attained equilibrium at 20 ns and 10 ns respectively, whereas the HC and CAPE complexes attained equilibrium before 5 ns itself (**Supplementary figure 2B**). The systems remained stable up to 50 ns and fluctuations were obtained in the range of 0.2 to 0.4Å for NS5 MTase Apo and the NS5 MTase complexes. These observations depict that the binding of molecules to nsP1 and NS5 proteins resulted in the formation of a stable complex.

Inhibition of CHIKV virus-specific MTase by HC and CAPE

To further validate the inhibition of viral methyltransferase activity of HC and CAPE, CHIKV nsP1 was purified and the MTase enzymatic activity of purified CHIKV nsP1 was performed using an indirect ELISA as per the previously published protocol [45][19][46]. Briefly, at 450 nm, the TMB/H2O2-ELISA substrate was used to identify immunoreactive proteins comprising the m7GMP-nsP1 complex. For IC_{50} calculations, the experiment was carried out by incubating CHIKV nsP1 protein (20 μM) in the reaction mixture with various concentrations of these two compounds. As the concentration of the compounds was increased, the absorbance or relative nsP1 activity was observed to be decreasing conforming to the inhibitory activity of both the compounds HC and CAPE against a viral MTase (Figure7). The dose-response curve showed the IC_{50} values for HC and CAPE are 86 nM and 9 nM respectively indicating these two compounds to be effective inhibitors of CHIKV nsP1.

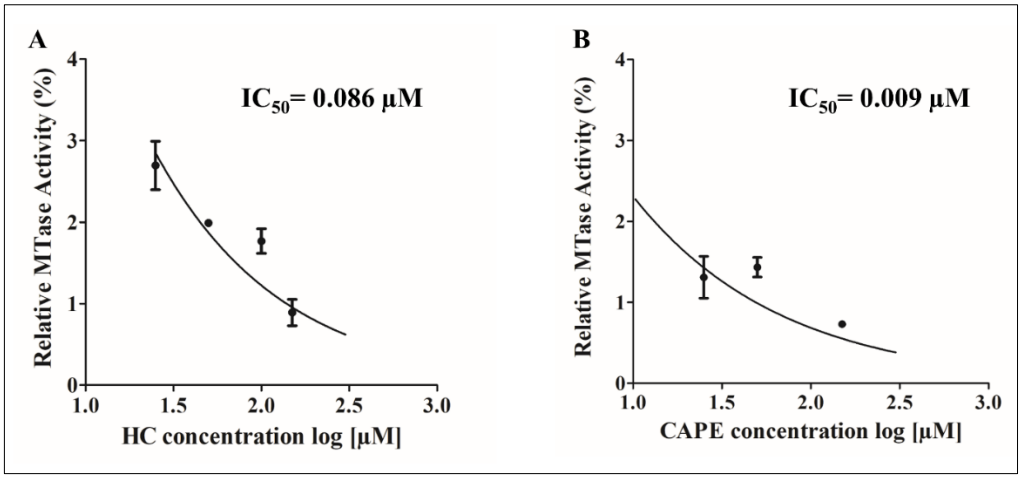

Figure 7: *ELISA based CHIKV nsP1 inhibition activity assay. The CHIKV nsP1 inhibition assay was executed in the presence of increasing concentration of HC (A) and CAPE (B) using an indirect ELISA assay. At 25 °C, the inhibitory activity assay was performed by adding 100 µM of SAM and 100 µM GTP along with 20 µM protein in each 50 µL reaction mixture of 50 mM Tris-HCl (pH 7.3), 10 mM NaCl, 2 mM* $MgCl_2$*, 5 mM DTT. The different concentration of inhibitors was added and incubated with the reaction mixture and ELISA assay was performed using anti-*m^7G *cap monoclonal antibody (Merck Millipore, Burlington, MA, USA). After that, an HRP-conjugated anti-mouse IgG1 secondary antibody (Affymetrix eBioscience, San Diego, CA, USA) was added to each well, along with 100 µL of TMB/H2O2-ELISA substrate (GeNei), and the absorbance readings (OD) at 450 nm were obtained using a multi-mode plate reader Cytation 3 (BioTek Instruments, Inc., Winooski, VT, USA). A decrease in absorbance with the increasing concentration of inhibitors was observed. The absorbance values represent an average of two readings plotted against the increasing concentration of the compounds. For normalisation, all of these readings were subtracted from the data obtained with reaction buffer only. Data points represent mean values, and error bars are standard deviations generated from duplicate experiments.*

Discussion

Communicable diseases transmitted through vectors such as mosquitoes remain a significant public health burden worldwide. Although human viruses belong to several viral families, *alphaviridae* and *flaviviridae* are the most significant burden on public health [4][6]. Drug development for mosquito-transmitted viruses such as DENV and CHIKV remains incomplete, and there is neither any commercially available drug to treat their infection nor a vaccine for these viruses. These viral pathogen's emergence and re-emergence poses a substantial health risk to the global human population. The current scarcity of vaccines and effective antivirals emphasizes the importance of developing new strategies to combat these life-threatening human pathogens.

Polyamines are ubiquitous molecules found in all cells at concentrations up to 1 mM. They play many important roles within the cell, including binding and altering the conformation of RNA, modifying transcription and translation rates, and affecting signaling pathways [12]. Similarly, they have an essential role in the viral life cycle as well. Previous studies showed that DFMO treatment cells depleted biogenic polyamine levels, leading to its antiviral activity against various viruses such as CHIKV, ZIKV, and DENV [11].

In this study, we have demonstrated that both HC and CAPE have significant anti-CHIKV and anti-DENV activity. It was well-thought-out that both of the compounds have potential for imminent progress as the outcomes result in better reduction for CHIKV and DENV infection when compared to the established positive control i.e.; DFMO in the plaque reduction assay. Surprisingly, the effective concentrations of both HC and CAPE were significantly lower than their toxic dose, i.e., EC_{50} values for both compounds are in the nanomolar and micromolar range for CHIKV and DENV respectively.

To quantify the copy number of viral RNA released from CHIKV and DENV infected cells, qRT-PCR was used that amplified the viral genome. qRT-PCR measures mRNA, which represents viral load during replication. Our finding shows that treatment with HC and CAPE

results in a significant reduction of viral load as compared to the positive control. The results were further validated by the IFA experiments.

Our findings supported a previously published concept that HC and CAPE are ODC inhibitors. HC is a naturally occurring flavonoid that is an established ODC inhibitor [25]. And CAPE is a natural ester that has also shown antiviral activity, and it significantly prevented the full induction of ODC by epidermal growth factor (EGF) [47]. In our study, both HC and CAPE molecules have shown more polyamine depletion as compared to the positive control. Furthermore, the exogenous polyamine addition assay did not rescue viral titre for CHIKV and DENV, implying that these compounds are acting also in ways other than the polyamine depletion pathways. Additionally, the results of bioinformatic prediction of both of the compounds show the binding energy in the range of -7.6 to 8 kcal/mol with the nsP1protein of CHIKV and NS5 of DENV, which are consistent with the results of CHIKV nsP1 biochemical assay.

Alphaviruses use an unconventional mechanism of RNA capping in which nsP1 plays a vital role in the capping of viral RNA, and the binding site of SAM and GTP remains conserved, as shown by MSA. Similarly, flaviviruses have a 5’ terminal cap 1 structure (m7GpppAmG), and SAM binding site remains conserved. Molecular docking of HC and CAPE showed promising results by exhibiting better binding than SAM and nearly equal to GTP. H-bond and hydrophobic interactions *in silico* show that essential residues required for the binding of SAM and GTP also bind to HC and CAPE. Hence, based on *in silico* evidence, it is hypothesized that these molecules will potentially bind to nsP1 and are suitable candidates for further testing. Moreover, the MTase inhibition assay further confirmed HC and CAPE binding to CHIKV nsP1. Furthermore, HC and CAPE have shown better binding results than SAM in the *in silico* study of NS5 MTase.

Conclusion

Our research offers a significant first report on the anti-CHIKV and anti-DENV capabilities of HC and CAPE through two mechanisms i.e. host-directed by depleting polyamines in mammalian cells and direct-antiviral agents targeting viral MTases. Given HC and CAPE's novel potential in limiting DENV and CHIKV infectivity, we suggest the need for further exploration as broad-spectrum antivirals for developing anti-DENV and anti-CHIKV therapeutics.

Acknowledgments

The authors are thankful to Department of biosciences and bioengineering, IIT Roorkee for central facilities. The authors thank the Macromolecular Crystallographic Facility (MCU) at IIC, Indian Institute of Technology, Roorkee. The authors would like to thank University Grants Commission (UGC) and Council of Scientific and Industrial Research (CSIR) and Ministry of Human Resource Development (MHRD) for providing financial support. This work was supported by a research grant of ST from ICMR Ref no. ISRM/12(46)/2020.

Ethical approval

DENV positive clinical sample was collected from HiTech Pathology Laboratory, Roorkee with the approval of the Institutional Human Ethical Committee (IHEC), Indian Institute of Technology, Roorkee (Ref no. BT/IHEC-IITR/2016/6499).

Authors contribution

MB, RR, AK, SM, BW, RK, VS conducted the experiments and analyzed the data. MB, RR, AK, SM, DS, PK and ST planned the experiments, analyzed the data, and wrote the manuscript.

Competing interests

The authors declare that they have no competing interests.

References

[1] M. G. Guzman, D. J. Gubler, A. Izquierdo, E. Martinez, and S. B. Halstead, “Dengue infection,” *Nat Rev Dis Primers*, vol. 2, Aug. 2016, doi: 10.1038/NRDP.2016.55.

[2] A. M. Powers *et al.*, “Evolutionary relationships and systematics of the alphaviruses,” *J Virol*, vol. 75, no. 21, pp. 10118–10131, Nov. 2001, doi: 10.1128/JVI.75.21.10118-10131.2001.

[3] “DENGUE/DHF SITUATION IN INDIA :: National Center for Vector Borne Diseases Control (NCVBDC).” https://nvbdcp.gov.in/index4.php?lang=1&level=0&linkid=431&lid=3715 (accessed Jan. 15, 2022).

[4] S. Bhatt *et al.*, “The global distribution and burden of dengue,” *Nature*, vol. 496, no. 7446, pp. 504–507, Apr. 2013, doi: 10.1038/NATURE12060.

[5] “CHIKUNGUNYA SITUATION IN INDIA :: National Center for Vector Borne Diseases Control (NCVBDC).” https://nvbdcp.gov.in/index4.php?lang=1&level=0&linkid=486&lid=3765 (accessed Jan. 15, 2022).

[6] “Geographical distribution of chikungunya virus disease cases reported worldwide, 2021.” https://www.ecdc.europa.eu/en/publications-data/geographical-distribution-chikungunya-virus-disease-cases-reported-worldwide-2021 (accessed Jan. 15, 2022).

[7] M. Kaur *et al.*, “Coinfection of chikungunya and dengue viruses: A serological study from North Western region of Punjab, India,” *Journal of Laboratory Physicians*, vol. 10, no. 4, p. 443, Oct. 2018, doi: 10.4103/JLP.JLP_13_18.

[8] H. S. Chahar, P. Bharaj, L. Dar, R. Guleria, S. K. Kabra, and S. Broor, “Co-infections with Chikungunya Virus and Dengue Virus in Delhi, India,” *Emerging Infectious Diseases*, vol. 15, no. 7, p. 1077, Jul. 2009, doi: 10.3201/EID1507.080638.

[9] S. Mahajan, S. Choudhary, P. Kumar, and S. Tomar, “Antiviral strategies targeting host factors and mechanisms obliging +ssRNA viral pathogens,” *Bioorg Med Chem*, vol. 46, Sep. 2021, doi: 10.1016/J.BMC.2021.116356.

[10] B. C. Mounce *et al.*, “Inhibition of Polyamine Biosynthesis Is a Broad-Spectrum Strategy against RNA Viruses,” *J Virol*, vol. 90, no. 21, pp. 9683–9692, Nov. 2016, doi: 10.1128/JVI.01347-16.

[11] B. C. Mounce *et al.*, “Interferon-Induced Spermidine-Spermine Acetyltransferase and Polyamine Depletion Restrict Zika and Chikungunya Viruses,” *Cell Host Microbe*, vol. 20, no. 2, pp. 167–177, Aug. 2016, doi: 10.1016/J.CHOM.2016.06.011.

[12] L. Miller-Fleming, V. Olin-Sandoval, K. Campbell, and M. Ralser, “Remaining Mysteries of Molecular Biology: The Role of Polyamines in the Cell,” *J Mol Biol*, vol. 427, no. 21, pp. 3389–3406, Oct. 2015, doi: 10.1016/J.JMB.2015.06.020.

[13] K. Igarashi and K. Kashiwagi, “Polyamines: Mysterious Modulators of Cellular Functions,” *Biochemical and Biophysical Research Communications*, vol. 271, no. 3, pp. 559–564, May 2000, doi: 10.1006/BBRC.2000.2601.

[14] K. J. Doyle, “Delayed, reversible hearing loss caused by difluoromethylornithine (DFMO),” *Laryngoscope*, vol. 111, no. 5, pp. 781–785, 2001, doi: 10.1097/00005537-200105000-00005.

[15] J. Jose, J. E. Snyder, and R. Kuhn, “A structural and functional perspective of alphavirus replication and assembly,” *Future Microbiol*, vol. 4, no. 7, pp. 837–856, 2009, doi: 10.2217/FMB.09.59.

[16] W. Filipowicz, Y. Furuichi, J. M. Sierra, S. Muthukrishnan, A. J. Shatkin, and S. Ochoa, “A protein binding the methylated 5’-terminal sequence, m7GpppN, of eukaryotic messenger RNA,” *Proc Natl Acad Sci U S A*, vol. 73, no. 5, pp. 1559–1563, 1976, doi: 10.1073/PNAS.73.5.1559.

[17] J. L. Hyde and M. S. Diamond, “Innate immune restriction and antagonism of viral RNA lacking 2’-O methylation,” *Virology*, vol. 479–480, pp. 66–74, May 2015, doi: 10.1016/J.VIROL.2015.01.019.

[18] T. Ahola and L. Kääriäinen, “Reaction in alphavirus mRNA capping: formation of a covalent complex of nonstructural protein nsP1 with 7-methyl-GMP.,” *Proc Natl Acad Sci U S A*, vol. 92, no. 2, p. 507, Jan. 1995, doi: 10.1073/PNAS.92.2.507.

[19] R. Mudgal, S. Mahajan, and S. Tomar, “Inhibition of Chikungunya virus by an adenosine analog targeting the SAM-dependent nsP1 methyltransferase,” *FEBS Letters*, vol. 594, no. 4, pp. 678–694, Feb. 2020, doi: 10.1002/1873-3468.13642.

[20] R. Jones, G. Bragagnolo, R. Arranz, and J. Reguera, “Capping pores of alphavirus nsP1 gate membranous viral replication factories,” *Nature*, vol. 589, no. 7843, p. 615, Jan. 2021, doi: 10.1038/S41586-020-3036-8.

[21] “Flaviviridae,” *Virus Taxonomy*, pp. 1003–1020, Jan. 2012, doi: 10.1016/B978-0-12-384684-6.00086-0.

[22] M. P. Egloff, D. Benarroch, B. Selisko, J. L. Romette, and B. Canard, “An RNA cap (nucleoside-2’-O-)-methyltransferase in the flavivirus RNA polymerase NS5: crystal structure and functional characterization,” *The EMBO Journal*, vol. 21, no. 11, p. 2757, Jun. 2002, doi: 10.1093/EMBOJ/21.11.2757.

[23] D. J. Kim *et al.*, “Herbacetin is a novel allosteric inhibitor of ornithine decarboxylase with antitumor activity,” *Cancer Res*, vol. 76, no. 5, p. 1146, Mar. 2016, doi: 10.1158/0008-5472.CAN-15-0442.

[24] L. R *et al.*, “Antiviral activity of selected flavonoids against Chikungunya virus,” *Antiviral Res*, vol. 133, pp. 50–61, Sep. 2016, doi: 10.1016/J.ANTIVIRAL.2016.07.009.

[25] H. Erdemli, S. Akyol, F. Armutcu, and O. Akyol, “Antiviral properties of caffeic acid phenethyl ester and its potential application,” *J Intercult Ethnopharmacol*, vol. 4, no. 4, p. 344, 2015, doi: 10.5455/JICE.20151012013034.

[26] B. T. Zhu, P. Wang, M. Nagai, Y. Wen, and H. W. Bai, “Inhibition of human catechol-O-methyltransferase (COMT)-mediated O-methylation of catechol estrogens by major polyphenolic components present in coffee,” *J Steroid Biochem Mol Biol*, vol. 113, no. 1–2, pp. 65–74, Jan. 2009, doi: 10.1016/J.JSBMB.2008.11.011.

[27] D. Xiang *et al.*, “Caffeic acid phenethyl ester induces growth arrest and apoptosis of colon cancer cells via the β-catenin/T-cell factor signaling,” *Anti-Cancer Drugs*, vol. 17, no. 7, pp. 753–762, Aug. 2006, doi: 10.1097/01.cad.0000224441.01082.bb.

[28] L. J. Chien, T. L. Liao, P. Y. Shu, J. H. Huang, D. J. Gubler, and G. J. J. Chang, “Development of real-time reverse transcriptase PCR assays to detect and serotype dengue viruses,” *J Clin Microbiol*, vol. 44, no. 4, pp. 1295–1304, Apr. 2006, doi: 10.1128/JCM.44.4.1295-1304.2006.

[29] A. C. Mishra *et al.*, “Stratified sero-prevalence revealed overall high disease burden of dengue but suboptimal immunity in younger age groups in Pune, India,” *PLoS Negl Trop Dis*, vol. 12, no. 8, Aug. 2018, doi: 10.1371/JOURNAL.PNTD.0006657.

[30] R. Kaur, Neetu, R. Mudgal, J. Jose, P. Kumar, and S. Tomar, “Glycan-dependent chikungunya viral infection divulged by antiviral activity of NAG specific chi-like lectin,” *Virology*, vol. 526, pp. 91–98, Jan. 2019, doi: 10.1016/J.VIROL.2018.10.009.

[31] R. Madhubala, “Thin-layer chromatographic method for assaying polyamines,” *Methods Mol Biol*, vol. 79, pp. 131–136, 1998, doi: 10.1385/0-89603-448-8:131.

[32] F. Sievers *et al.*, “Fast, scalable generation of high-quality protein multiple sequence alignments using Clustal Omega,” *Mol Syst Biol*, vol. 7, 2011, doi: 10.1038/MSB.2011.75.

[33] Structural insights into viral RNA capping and plasma membrane targeting by Chikungunya virus nonstructural protein 1. Cell Host & Microbe, 29(5), 757–764.e3 | 10.1016/j.chom.2021.02.018.” https://sci-hub.se/https://doi.org/10.1016/j.chom.2021.02.018 (accessed Jan. 20, 2022).

[34] R. Jones, G. Bragagnolo, R. Arranz, and J. Reguera, “Capping pores of alphavirus nsP1 gate membranous viral replication factories,” *Nature 2020 589:7843*, vol. 589, no. 7843, pp. 615–619, Dec. 2020, doi: 10.1038/s41586-020-3036-8.

[35] A. Waterhouse *et al.*, “SWISS-MODEL: homology modelling of protein structures and complexes,” *Nucleic Acids Res*, vol. 46, no. W1, pp. W296–W303, Jul. 2018, doi: 10.1093/NAR/GKY427.

[36] O. Trott and A. J. Olson, “AutoDock Vina: improving the speed and accuracy of docking with a new scoring function, efficient optimization and multithreading,” *J Comput Chem*, vol. 31, no. 2, p. 455, 2010, doi: 10.1002/JCC.21334.

[37] S. Dallakyan and A. J. Olson, “Small-molecule library screening by docking with PyRx,” *Methods Mol Biol*, vol. 1263, pp. 243–250, 2015, doi: 10.1007/978-1-4939-2269-7_19.

[38] N. M. O’Boyle, M. Banck, C. A. James, C. Morley, T. Vandermeersch, and G. R. Hutchison, “Open Babel: An Open chemical toolbox,” *Journal of Cheminformatics*, vol. 3, no. 10, pp. 1–14, Oct. 2011, doi: 10.1186/1758-2946-3-33/TABLES/2.

[39] Y. Zhao *et al.*, “A Crystal Structure of the Dengue Virus NS5 Protein Reveals a Novel Inter-domain Interface Essential for Protein Flexibility and Virus Replication,” *PLoS Pathogens*, vol. 11, no. 3, pp. 1–27, Mar. 2015, doi: 10.1371/JOURNAL.PPAT.1004682.

[40] B. Zhao *et al.*, “Structure and function of the Zika virus full-length NS5 protein,” *Nature Communications 2017 8:1*, vol. 8, no. 1, pp. 1–9, Mar. 2017, doi: 10.1038/ncomms14762.

[41] “PyMOL | pymol.org.” https://pymol.org/2/ (accessed Mar. 05, 2022).

[42] R. A. Laskowski and M. B. Swindells, “LigPlot+: multiple ligand-protein interaction diagrams for drug discovery,” *J Chem Inf Model*, vol. 51, no. 10, pp. 2778–2786, Oct. 2011, doi: 10.1021/CI200227U.

[43] D. Van Der Spoel, E. Lindahl, B. Hess, G. Groenhof, A. E. Mark, and H. J. C. Berendsen, “GROMACS: fast, flexible, and free,” *J Comput Chem*, vol. 26, no. 16, pp. 1701–1718, Dec. 2005, doi: 10.1002/JCC.20291.

[44] A. W. Schüttelkopf and D. M. F. Van Aalten, “PRODRG: a tool for high-throughput crystallography of protein-ligand complexes,” *Acta Crystallogr D Biol Crystallogr*, vol. 60, no. Pt 8, pp. 1355–1363, Aug. 2004, doi: 10.1107/S0907444904011679.

[45] S. Tomar, M. Narwal, E. Harms, J. L. Smith, and R. J. Kuhn, “Heterologous production, purification and characterization of enzymatically active Sindbis virus nonstructural protein nsP1,” *Protein Expr Purif*, vol. 79, no. 2, pp. 277–284, Oct. 2011, doi: 10.1016/J.PEP.2011.05.022.

[46] R. Kaur, R. Mudgal, M. Narwal, and S. Tomar, “Development of an ELISA assay for screening inhibitors against divalent metal ion dependent alphavirus capping enzyme,” *Virus Res*, vol. 256, pp. 209–218, Sep. 2018, doi: 10.1016/J.VIRUSRES.2018.06.013.

[47] Z. S. Zheng, G. Z. Xue, D. Grunberger, and J. H. Prystowsky, “Caffeic acid phenethyl ester inhibits proliferation of human keratinocytes and interferes with the EGF regulation of ornithine decarboxylase.,” *Oncology Research*, vol. 7, no. 9, pp. 445–452, Jan. 1995, Accessed: May 19, 2022. [Online]. Available: https://europepmc.org/article/med/8835288